



HAL
open science

An Ensemble Kalman Filter for severe dust storm data assimilation over China

C. Lin, Z. Wang, J. Zhu

► **To cite this version:**

C. Lin, Z. Wang, J. Zhu. An Ensemble Kalman Filter for severe dust storm data assimilation over China. Atmospheric Chemistry and Physics, 2008, 8 (11), pp.2975-2983. hal-00296571

HAL Id: hal-00296571

<https://hal.science/hal-00296571>

Submitted on 18 Jun 2008

HAL is a multi-disciplinary open access archive for the deposit and dissemination of scientific research documents, whether they are published or not. The documents may come from teaching and research institutions in France or abroad, or from public or private research centers.

L'archive ouverte pluridisciplinaire **HAL**, est destinée au dépôt et à la diffusion de documents scientifiques de niveau recherche, publiés ou non, émanant des établissements d'enseignement et de recherche français ou étrangers, des laboratoires publics ou privés.

An Ensemble Kalman Filter for severe dust storm data assimilation over China

C. Lin^{1,2}, Z. Wang¹, and J. Zhu¹

¹LAPC and NZC, Institute of Atmospheric Physics, Chinese Academy of Sciences, Beijing, China

²Graduate University of Chinese Academy of Sciences, Beijing, China

Received: 17 September 2007 – Published in Atmos. Chem. Phys. Discuss.: 3 December 2007

Revised: 8 May 2008 – Accepted: 14 May 2008 – Published: 17 June 2008

Abstract. An Ensemble Kalman Filter (EnKF) data assimilation system was developed for a regional dust transport model. This paper applied the EnKF method to investigate modeling of severe dust storm episodes occurring in March 2002 over China based on surface observations of dust concentrations to explore the impact of the EnKF data assimilation systems on forecast improvement. A series of sensitivity experiments using our system demonstrates the ability of the advanced EnKF assimilation method using surface observed PM₁₀ in North China to correct initial conditions, which leads to improved forecasts of dust storms. However, large errors in the forecast may arise from model errors (uncertainties in meteorological fields, dust emissions, dry deposition velocity, etc.). This result illustrates that the EnKF requires identification and correction model errors during the assimilation procedure in order to significantly improve forecasts. Results also show that the EnKF should use a large inflation parameter to obtain better model performance and forecast potential. Furthermore, the ensemble perturbations generated at the initial time should include enough ensemble spreads to represent the background error after several assimilation cycles.

1 Introduction

Dust storms have drawn much concern during the past two decades for the various impacts on atmospheric environment, biogeochemical cycles, radiative balance and human health. In recent years, many observational programs have been carried out to study Asian dust storms, and much progress has been achieved and improved the understanding of climatic

and synoptic features of soil dust aerosols (Murayama et al., 2001; Mori et al., 2002; Sugimoto, 2002; Sugimoto et al., 2002; Zhang et al., 2003). On the other hand, in order to provide high spatial and temporal resolution forecasts of Asian dust and reproduce many important observational facts, several numerical models have been developed and used to study the deflation, transport and budget of soil dust over East Asia (Wang et al., 2000; Shao, 2001; Song et al., 2001; Uno et al., 2001; Gong et al., 2003; Shao et al., 2003; Park et al., 2003; Liu et al., 2003; Han et al., 2004). The intercomparison study (DMIP) involving eight dust emission/transport models over Asia found that the model results correctly captured the major dust onset and cessation timing at each observation site. However, the maximum concentrations predicted by each model differed by 2–4 times (Uno et al., 2006), clearly indicating that modeling results of dust storms with these models are significantly model dependent.

Numerical forecasts of dust storms suffer from uncertainties both in initial conditions and in the model itself. Simply comparing model forecasts to observations cannot separate these uncertainties. Using a data assimilation technique we can firstly reduce uncertainty of initial conditions that may lead to improved forecasts and secondly better examine model errors through comparison with observations, since the uncertainty of initial conditions can be maximally reduced by assimilation of observations at initial times. Vautard et al. (2004) investigated the potential of data assimilation of surface ozone concentrations in a chemistry-transport model over the European continent using statistical interpolation and showed that both the analyses and the 1~2 day forecast are improved. Recently, Yumimoto et al. (2007) applied a four-dimensional variation (4DVAR) to a regional dust model to assimilate NIES Lidar observations over East Asia to inverse Asian dust emissions demonstrating better estimation capability. Niu et al. (2007) developed a 3DVAR using satellite retrieved dust loading and surface visibility in



Correspondence to: Z. Wang
(zifawang@mail.iap.ac.cn)

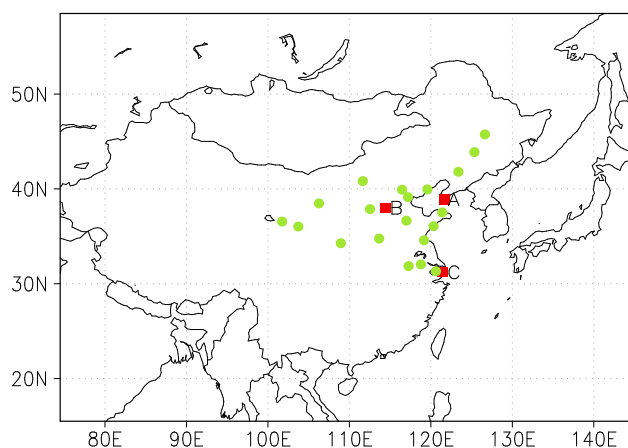


Fig. 1. The model domain and the observational network. The closed circles indicate positions of those PM_{10} observations used in assimilation cycles on 22 March, while the rectangles are those used for independent verifications.

the CUACE/Dust forecast system and showed the capability of short-term forecast improvement. These all indicate the important role of data assimilation to combine observations with modeling in air quality prediction. In these methods, the background error statistics, one of the most important aspects of data assimilation, are usually assumed to be spatially homogeneous, horizontally isotropic, and temporally stationary. This assumption may disagree with the actual errors which may have significant flow-dependence, especially for meso-scale motions. Although the background error statistics can evolve implicitly in 4DVAR during the time window, the complexity of constructing the adjoint matrix and the expensive computation in 4DVAR usually prevent it from common application especially for complicated models. Hanea et al. (2007) used a hybrid Kalman filter algorithm combining the reduced-rank square root (RRSQRT) and the ensemble Kalman filter (EnKF) for ozone simulation in the European Operational Smog (EUROS) atmospheric chemistry transport model. The hybrid algorithm combines the best of both filters with more than 30 model evaluations.

In this study we perform ensemble Kalman filter (EnKF) data assimilation experiments during some severe dust storm episodes in China using surface observations of dust concentrations and a realistic model in order to explore the impacts on forecast skills. The EnKF is an advanced and flexible technique for data assimilation which can calculate flow-dependent statistics from the ensemble forecasts and have been widely used in atmospheric and oceanic applications (Evensen, 1994; Houtekamer and Mitchell, 1998, 2001; Mitchell and Houtekamer, 2000, 2002; Houtekamer et al., 2005; Whitaker et al., 2002; Lorenc, 2003; Evensen, 2003, 2006; Hanea et al., 2007). However the EnKF has not been applied in severe dust storm forecasts. In this study, we made an initial effort to explore the potential problems of this issue with EnKF.

Table 1. Number of valid PM_{10} observations after quality control over North China during 15–25 March 2002.

Date	15	16	17	18	19	20	21	22	23	24	25
No. of Obs.	0	6	16	10	11	12	17	23	8	4	0

2 Data source and model description

2.1 Data

Daily averaged PM_{10} (suspended particles with aerodynamic diameter measuring $10\ \mu\text{m}$ or less) concentrations observed by the State Environmental Protection Administration, China (SEPA) from 15 March 2002 to 25 March 2002 are used for assimilation and validation. PM_{10} observations reflect not only dust aerosols but also anthropogenic aerosols. Before they are used, the PM_{10} observations are selected according to the 3-h surface synoptic observations of dust events from the China Meteorological Administration (CMA). If there is at least one occurrence of floating dust phenomenon observed at stations located within 1 latitude degree around the PM_{10} station during the day, the contribution of PM_{10} observations of this station are considered as mainly coming from dust, and thus selected for assimilation and validation. Otherwise the data would be discarded. The number of qualified PM_{10} observations after quality control is listed in Table 1, clearly indicating irregular sampling of dust storms. Figure 1 presents the distribution of observation sites (green dots) passing through quality control and used for assimilation on 22 March, and the red rectangles represent three selected independent sites that are only used for verification. The Lidar observation at Beijing was performed at the Sino-Japan Friendship Center for Environmental Protection during the same period (Sugimoto et al., 2003). The visibility observations are the surface observations from the China Meteorological Administration (CMA).

2.2 Model description and setting

The regional dust transport model (Wang et al., 2000) included deflation, transport, diffusion, and removal processes during the life cycle of the yellow sand particles. This model had been successfully used to study atmospheric trace gases and particles, such as SO_x , dust, O_3 and acid rain over East Asia (Wang et al., 2000, 2002; Uematsu et al., 2003). The advanced deflation module of yellow sand has been designed after detailed analysis of the meteorological conditions, landform, and climatology from daily weather report at about 300 local weather stations in north China. Details about the model are described by Wang et al. (2000). The simulation domain used ranges from (75°E , 16°N) to (146°E , 60°N) consisting of 72 by 45 horizontal grid cells and 18 vertical layers as shown in Fig. 1.

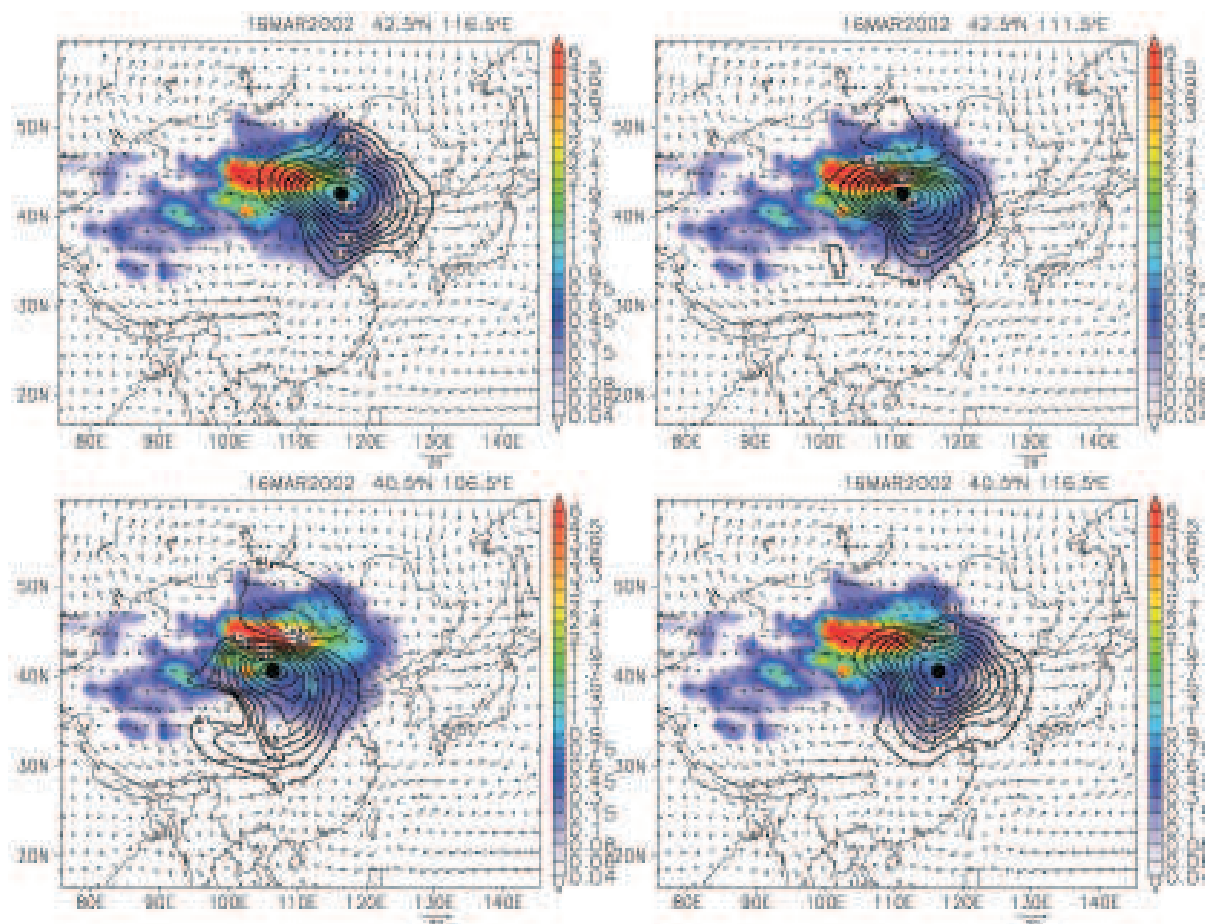


Fig. 2. Correlations (line contours) of surface concentrations with those at different points denoted by the black dots directly estimated from ensemble perturbations at 03:00 UTC on 16 March 2002. The shaded areas show the simulated surface concentrations of dust particles.

A heavy dust storm occurred in northern China and reached Beijing on 20 March 2002, with peak concentration of Total Suspended Particles (TSP) reaching 10.9 mg m^{-3} , 54 times higher than the National Air Quality Standard of China (Sun et al., 2004). Model analysis with Lidar observation of this dust storm in Beijing revealed the source and transport path of the dust and further explained the reasons for the occurrence of such extremely high dust concentrations (Sugimoto et al., 2003). It not only swept over most parts of China but also reached Korea and Japan. Using model simulation, Park et al. (2003) studied dust emissions from the source areas of it. In addition, Shao et al. (2003) simulated it with an integrated modeling system and found the model could accurately predict the spatial pattern and temporal evolution of dust concentration. Han et al. (2004) developed a size-segregated aerosol model and coupled this with a regional air quality model to simulate the dust storms of 15–24 March 2002. In this study, we developed a regional chemical transport model combined with EnKF data assimilation method to improve the forecast performance and to investigate the vertical structure of this super dust storm during the period of 15–25 March 2002 in East Asia.

3 Data assimilation with Ensemble Kalman Filter

The basic idea of the EnKF (Evensen, 1994) is to construct a Monte Carlo ensemble such that the mean of the ensemble is the best estimate, and the ensemble error covariance is a good estimate of the forecast error covariance.

At the current assimilation time t (for notational simplicity, the t time subscript will be dropped), we assume that we have an ensemble of forecasts that randomly sample the forecast errors, denoted by $\mathbf{x}_1^b, \mathbf{x}_2^b, \dots, \mathbf{x}_m^b$. The ensemble mean is defined by $\bar{\mathbf{x}}^b = m^{-1} \sum_{i=1}^m \mathbf{x}_i^b$. The ensemble perturbation from the mean for the i -th member is $\mathbf{x}_i^b = \mathbf{x}_i^b - \bar{\mathbf{x}}^b$.

The EnKF performs an ensemble of similar assimilation cycles, $i=1, \dots, m$, with each member updated to a different realization of the observations:

$$\mathbf{x}_i^a = \mathbf{x}_i^b + \hat{\mathbf{K}} \left(\mathbf{y}_i - H(\mathbf{x}_i^b) \right), \quad (1)$$

where H is the observation operator that maps the model states to the observation space. In Eq. (1), $\mathbf{y}_i \approx N(0, \mathbf{R})$ is a perturbed observations from observations \mathbf{y} , and \mathbf{R} is the

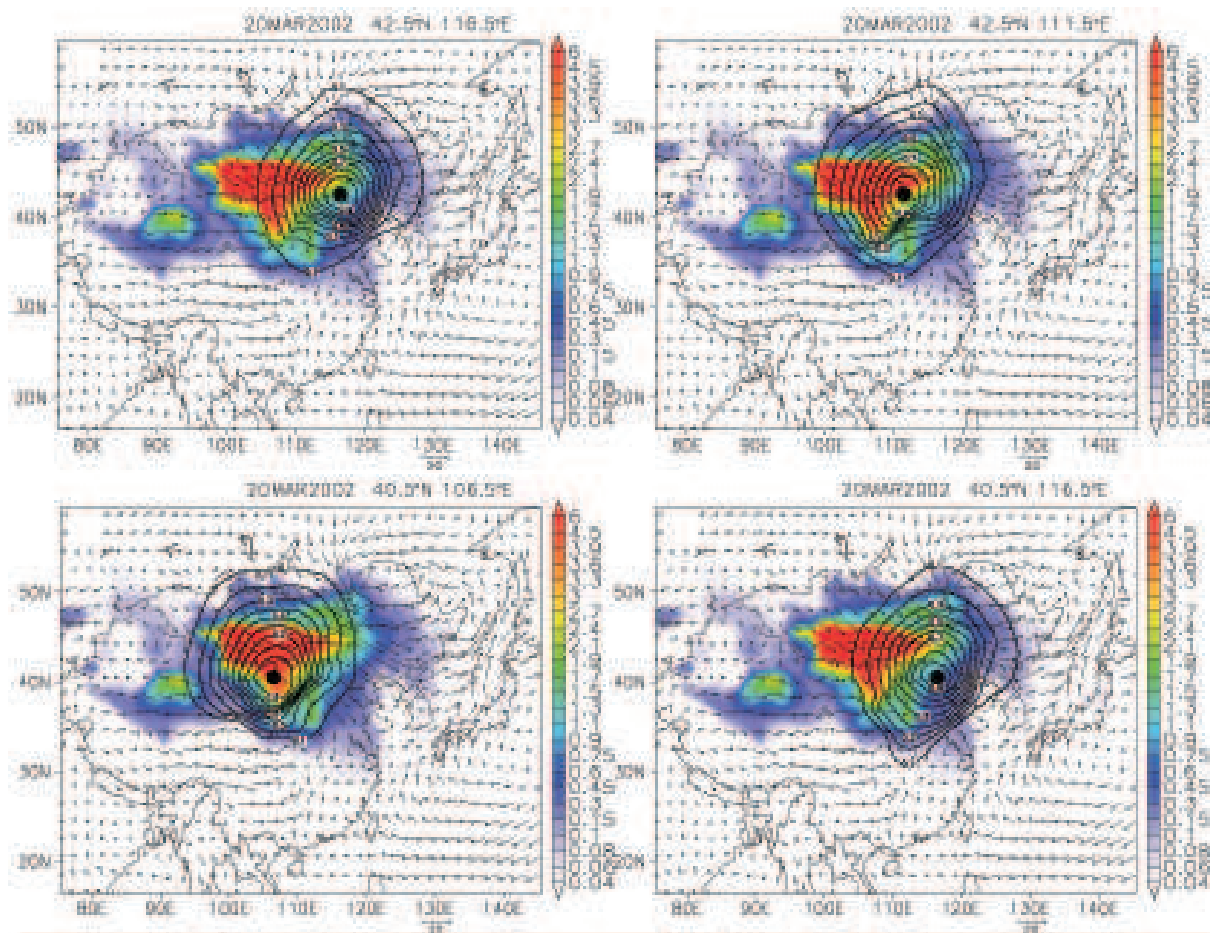


Fig. 3. As in Fig. 2, but at 03:00 UTC on 20 March 2002.

observation error covariance which is diagonal with variance equal to 10% of the value of \mathbf{y} . The gain matrix $\hat{\mathbf{K}}$ is defined as

$$\hat{\mathbf{K}} = \hat{\mathbf{P}}^b \mathbf{H}^T (\mathbf{H} \hat{\mathbf{P}}^b \mathbf{H}^T + \mathbf{R})^{-1}. \quad (2)$$

It can be formed without ever explicitly estimating and storing the full forecast error covariance $\hat{\mathbf{P}}^b$, but by using the following equations to calculate $\hat{\mathbf{P}}^b \mathbf{H}^T$ and $\mathbf{H} \hat{\mathbf{P}}^b \mathbf{H}^T$ directly (Evensen, 1994, Houtekamer and Mitchell, 1998):

$$\hat{\mathbf{P}}^b \mathbf{H}^T = \frac{1}{m-1} \sum_{i=1}^m \mathbf{x}_i^b (H(\mathbf{x}_i^b) - \overline{H(\mathbf{x}^b)})^T, \quad (3)$$

$$\mathbf{H} \hat{\mathbf{P}}^b \mathbf{H}^T = \frac{1}{m-1} \sum_{i=1}^m (H(\mathbf{x}_i^b) - \overline{H(\mathbf{x}^b)}) (H(\mathbf{x}_i^b) - \overline{H(\mathbf{x}^b)})^T. \quad (4)$$

In Eqs. (3) and (4),

$$\overline{H(\mathbf{x}^b)} = \frac{1}{m} \sum_{i=1}^m H(\mathbf{x}_i^b).$$

Once each member is updated, we take the analyzed ensemble mean $\bar{\mathbf{x}}^a = m^{-1} \sum_{i=1}^m \mathbf{x}_i^a$ as the optimal analysis.

In this study, the initial background ensemble perturbations are generated by adding random amplitude and phase shifts to the first-guess $\mathbf{x}(x, y, z)$ as follows:

$$\mathbf{x}_i(x, y, z) = (1 + \delta_i) \mathbf{x}(x + \varepsilon_i, y + \omega_i, z + \eta_i)$$

where,

$$\delta \in N(0, a^2), \varepsilon \in N(0, l_x^2), \omega \in N(0, l_y^2), \eta \in N(0, l_z^2).$$

l_x , g_f , l_y and l_z represent the standard deviations of the phase perturbations and are assumed to be about 200 km in this study, while the amplitude perturbation a is assumed to be 20% of the first guess. In order to prevent the usage of negative values, we generate a using an exponential function as

$$a = e^{\left(\gamma \times sd - \frac{1}{2} \times sd^2\right)}$$

where γ is randomly drawn from a normal distribution with zero mean and variance equal to 1, and sd is equal to 20%.

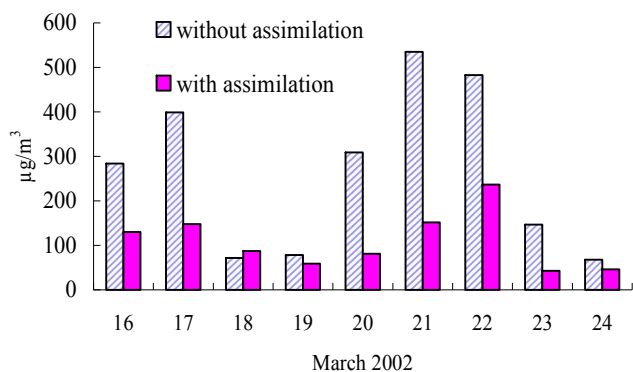


Fig. 4. Comparison of the root mean square (RMS) error between observed daily-mean PM_{10} levels and predicted 24 h-averaged dust aerosol concentrations ($d < 10 \mu\text{m}$) without assimilation (line rectangle) and the analyses of EnKF assimilation (shaded rectangle) at three independent validation sites during 16–24 March 2002. The 10-day assimilation cycle is used for EnKF analysis.

A parameter $\alpha \geq 1$ is introduced to allow for inflation of the forecast error variance since the ensemble spread itself may be too small to draw the model states to the observations. In this case, Eq. (2) will be rewritten as

$$\mathbf{K} = \alpha \mathbf{P}^b \mathbf{H}^T (\alpha \mathbf{H} \mathbf{P}^b \mathbf{H}^T + \mathbf{R})^{-1}. \quad (5)$$

In the study here, the parameter α increases with time from 1 to 640 (estimated according to the likely minimal root mean square error).

In addition, the value for dust concentrations should be positive. Therefore, the analysis would be set to be zero if it is negative.

4 Results

Two sets of model runs with and without the assimilation schemes addressed above were performed to test the performance of the EnKF used in the regional transport model of dust. Firstly, the tests were performed once a day during 15–25 March 2002 with initial perturbations generated on 03:00 UTC, 15 March to check the overall impact of the assimilation on 24-h forecasts.

To give an impression of the anisotropic nature of the horizontal correlations, we present some examples of horizontal correlations of surface concentrations with respect to the points shown with the black dots in Figs. 2 and 3. The correlations are directly estimated from 50-member ensembles on 03:00 UTC, 16 and 20 March. It can be seen that the spatial structures are dependent on the flow which displays the most important property of EnKF compared to other traditional data assimilation methods such as optimal interpolation (OI) and three-dimension variational assimilation (3D-Var). In OI and 3D-Var algorithms, the statistics in background error co-

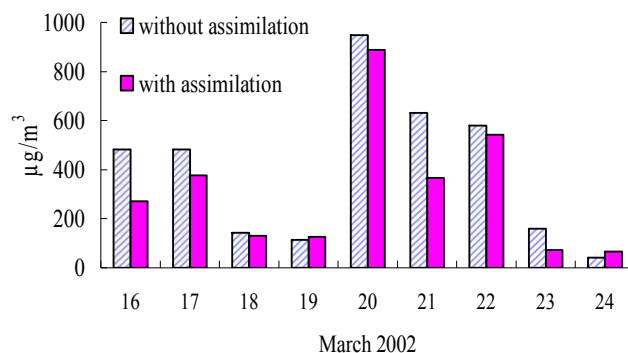


Fig. 5. Similar to Fig. 4, but for the 24 h-averaged predictions without (line rectangle) and with (shaded rectangle) assimilation at all observational sites when the observations pass through quality control.

variance are generally taken to be isotropic and largely homogeneous with little variation in time, which is not consistent with the real systems.

The root mean square (RMS) errors between daily averaged PM_{10} observations and the simulated 24 h-averaged forecasts ($d < 10 \mu\text{m}$) without assimilation (line rectangle) and the analyses with EnKF assimilation (shaded rectangle) at three independent observation stations were calculated during 16–25 March 2002 (Fig. 4). It can be seen that the RMS errors of the assimilated results are much smaller than that without assimilation totally, which clearly shows the potential ability of the EnKF method used in the regional transport model. The RMS errors of the 24 h-averaged forecasts without (line rectangle) and with (shaded rectangle) assimilation for all sites are shown in Fig. 5. The difference between observations and the 24 h forecasts with assimilation are smaller than those without assimilation, showing that the forecasts are also improved after EnKF assimilation, but not obviously for the whole area.

An independent Lidar observed the dust extinction coefficients in Beijing in the same period. Figure 6 gives a comparison between Lidar observations and the modeled dust extinction coefficient with and without assimilation. These results illustrate that use of the EnKF method solely assimilating surface PM_{10} concentration changed the vertical structures of dust distribution and significantly improved the modeling results in Beijing compared with Lidar observations. Two peaks of dust concentration distribution exhibited on 20 March in Beijing with EnKF assimilation agree well with the observed dust extinction coefficients near the surface. For higher layers about 500–1000 m above the ground, it is possible that observations on 20 March might be missing because the dust layer is too thick. This prevents the penetration of the lidar signal, so that we cannot compare the results in detail. Generally speaking, the vertical distribution after assimilation is improved with the RMS error reduced (Fig. 6d) and the correlation a little increase (Fig. 6e). This may be largely

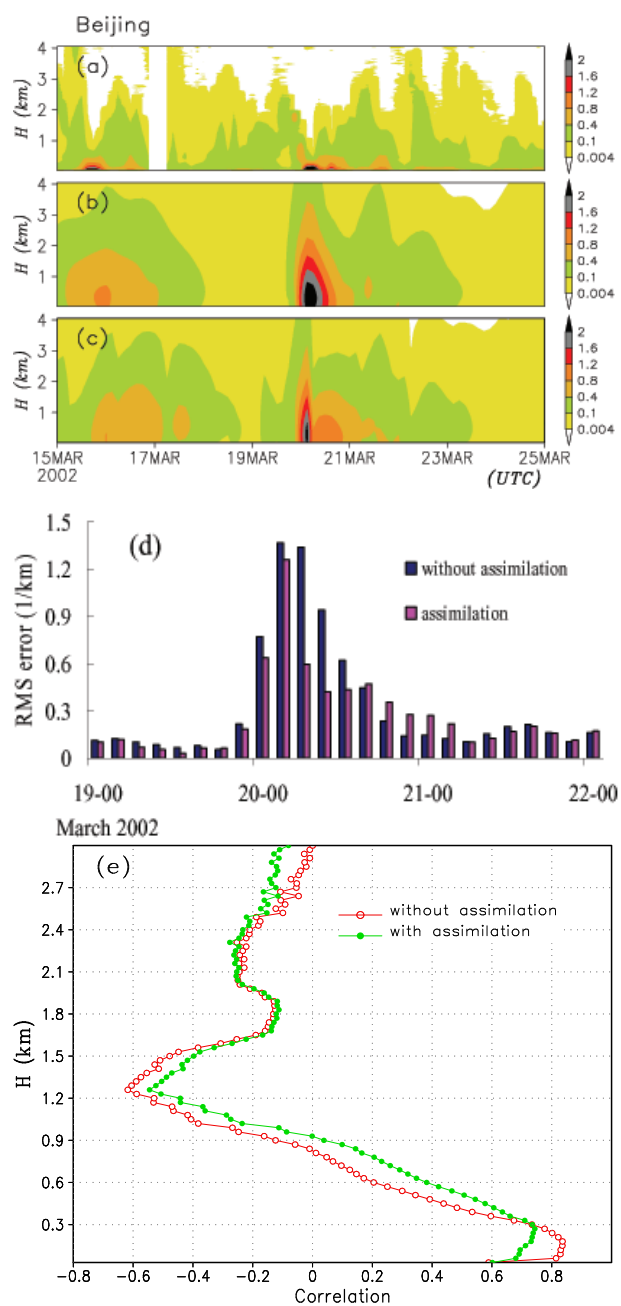


Fig. 6. Comparison of Lidar observed (a) and predicted dust extinction coefficient (unit: 1/km) without (b) and with (c) assimilation in Beijing during 15–24 March 2002. Comparison of the root mean square error (d) and correlation (e) between observations and predictions below 3 km with and without assimilation in Beijing during 00:00 UTC, 19 March to 00:00 UTC 22 March 2002.

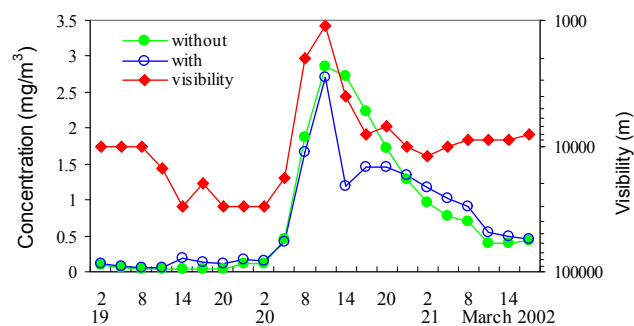


Fig. 7. Time series of surface concentrations of dust aerosols with (blue solid line) and without (green dashed line) EnKF assimilation and visibility in Beijing during 19–21 March 2002.

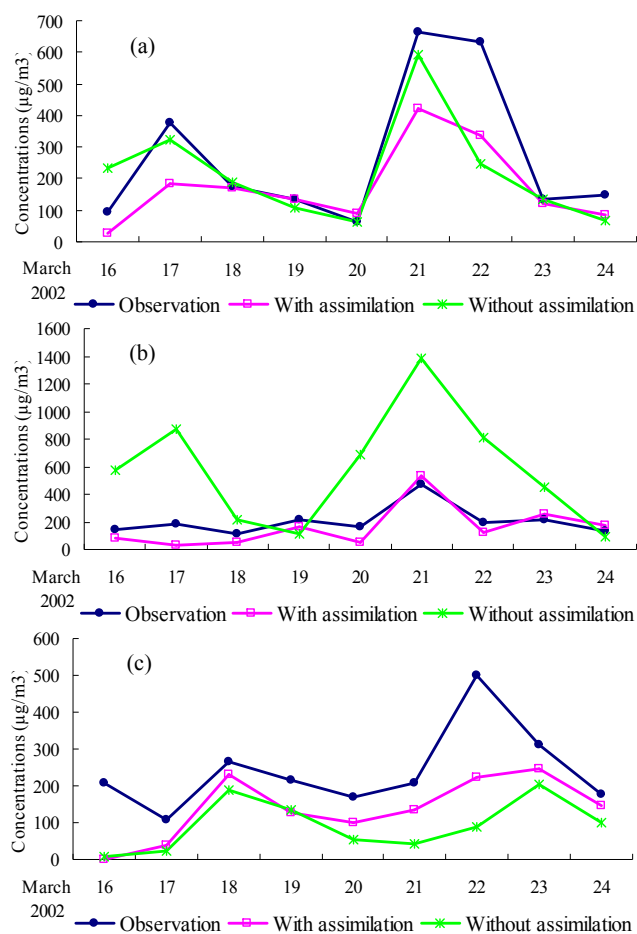


Fig. 8. Comparisons of assimilation results and simulation with observed daily-mean PM₁₀ observations at three independent observation stations, respectively.

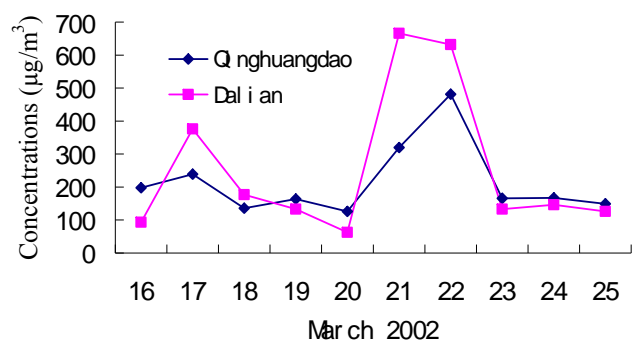


Fig. 9. Variations of observed PM₁₀ at Dalian and Qinhuangdao during 16–15 March 2002.

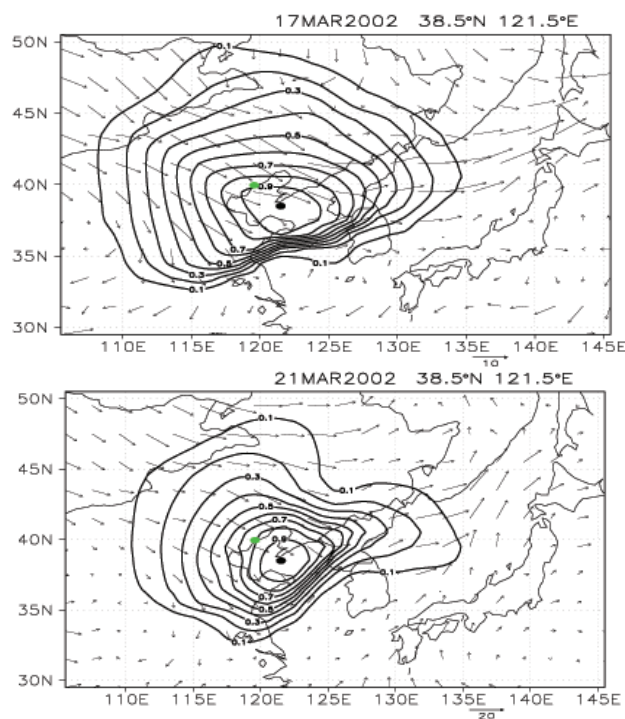


Fig. 10. As in Fig. 2 but with respect to Dalian site on 17 March (top panel) and 21 March (bottom one). The black dot and the green dot are the locations of Dandian and Qinhuangdao, respectively.

due to the vertical structure in background error covariance calculated from the ensemble, which propagates the surface PM₁₀ observations to high levels.

Surface dust concentrations and visibility at 3 h intervals are compared in Beijing in Fig. 7. On 20 March, the two troughs of visibility correspond to the two peaks of dust concentrations with assimilation but just one peak of the simulated results without assimilation, with the bigger trough corresponding to the higher peak. This clearly demonstrates the important role of the ensemble Kalman filter plays. The correlation between the 3 h surface visibility and dust concentrations during the period of 20–21 March is -0.69 without

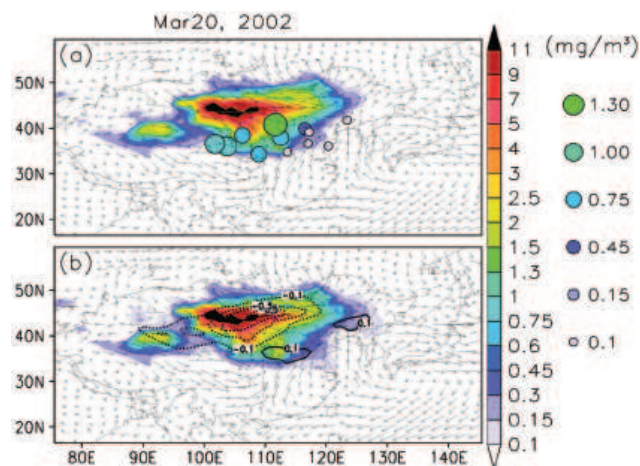


Fig. 11. Surface distribution of dust concentration over East Asia without (a) and with (b) assimilation on 20 March 2002. The contours show the difference between situations with and without assimilation. The colored circles represented the observed PM₁₀ (mg/m^3).

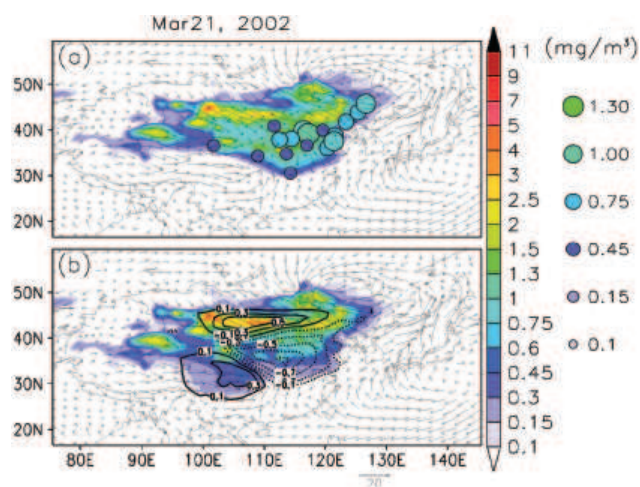


Fig. 12. As in Fig. 11, but on 21 March 2002.

assimilation and -0.73 with assimilation, which exceed the significance of 99%. Figure 8 shows the assimilated results of surface dust aerosols ($d < 10 \mu\text{m}$) with assimilation once a day at three independent observed stations, respectively (a, b, c as shown in Fig. 1). It shows that the assimilation analyses are closer to the observations than in the simulation without EnKF assimilation, especially at Shijiazhuang (b) and Shanghai (c). The assimilated results in Dalian (a) are not so close to the observations as the simulation, which may be due to the low resolution of the model. If the model resolution is relatively high the assimilated results are better, such as the results of (b) and (c).

We here select point A (Dalian) to explain the important of resolution. For Dalian, the analyses on 17 and 21 March are worse than in the simulation, while the others are comparable to the simulation. From Fig. 9 we can see that the variation of observed PM_{10} at two nearby points (Dalian and Qinghuangdao) are quite different, especially on 17 March and 21 March, indicating that spatial variability of the dust storm is very strong and the correlation coefficient is in fact small. However, the resolution of model is $1^\circ \times 1^\circ$, which may be too low to resolve the spatial variability of such processes, and then the dust concentrations calculated from the model are similarly distributed in a relatively large region. So the correlations estimated directly from the ensemble forecasts are distributed in a relatively large region, which does not agree with the actual one, so it can bias the assimilated results. Figure 10 gives the correlation distribution of Dalian on 17 March (upper panel) and 21 March (bottom panel), in which the black dot and the green dot denote the position of Dalian and Qinghuangdao respectively. We can see that the correlation coefficients of these two points are larger than 0.8. Therefore, the method to solve it is to increase the model resolution.

Figures 11 and 12 give surface distribution of 24 h-averaged dust concentration over East Asia without (a) and with assimilation (b) on 20–21 March, respectively. The contours show the difference between situations with and without assimilation. Compared with the PM_{10} observations, the forecast concentrations on 20 March are much larger than the observations, especially in the north part of North China, while smaller in the south part. After EnKF assimilation, the average of one-day forecast concentrations decreases in the north part and increases in the south part of North China. On 21 March, the forecasts after assimilation decrease in the middle and south part and increase in north and southwest part of North China. Overall, the EnKF assimilation compensates the model deficiency and improves the forecasts.

5 Conclusion and discussion

The correlation patterns of several selected points shown in Figs. 2 and 3 prove that EnKF can calculate the flow-dependent statistics which may not be expected in other traditional assimilation techniques. To use surface PM_{10} observations for data assimilation of dust storms, it is necessary to select them according to the surface synoptic dust event reports. This study shows that, using advanced methods such as EnKF, the assimilation of surface PM_{10} observations can provide better initial conditions and lead to improved forecasts of dust storms. However, the forecasts still have much room for improvement. First, the current PM_{10} observations that are reported to SEPA are only daily-averaged. For fast changing processes such as dust storms, this study shows that much more frequent observations are needed to correctly describe the fast evolution structure. Denser observational

networks are also necessary to specify the spatial variability of such processes as air pollution (see Fig. 8). Second, the model errors are the main contributors to forecast errors, at least in some regions. The assimilation can provide good initial conditions, but a forecast with large errors can result from model errors (see Fig. 5). Therefore, significant improvement of forecasts it requires identification and correction model errors during the assimilation procedure. This may be achieved by either four-dimensional variation method or augmented EnKF. This should be a priority for further studies in this direction.

The dust concentrations vary very rapidly and are generally independent in different dust process. Therefore, the ensemble perturbations generated at the initial time may not have enough ensemble spread to represent the background error after several assimilation cycles. In this study we found it is necessary to use a large inflation parameter (α defined in Eq. (5)). In future study, we will try our best to specify the model errors (e.g. errors in meteorological fields, dust emissions, dry deposition velocity) to overcome this limitation. In addition, we also found that the analysis may have negative values for dust concentrations. We use a simple approach that sets negative values to zero. More skillful methods should be explored in further studies.

Acknowledgements. This study was supported by Chinese Academy of Sciences (KZCX3-SW-202 and KZCX2-YW-205), the Natural Science Foundation of China (40775077/40533017) and the National 863 project (20060106A3004). We are appreciative of N. Sugimoto for providing the Lidar data, the SEPA for providing observed PM_{10} data and Raleigh Martin at the Princeton University for English improvements.

Edited by: F. J. Dentener

References

- Evensen, G.: Sequential data assimilation with a nonlinear quasi-geostrophic model using Monte Carlo methods to forecast error statistics, *J. Geophys. Res.*, 99, 10 143–10 162, 1994.
- Evensen, G.: The Ensemble Kalman Filter: Theoretical Formulation and Practical Implementation, *Ocean Dynamics*, 53, 343–367, 2003.
- Evensen, G.: Data Assimilation: The Ensemble Kalman Filter, Springer, German, 2006.
- Gong, S. L., Zhang, X. Y., Zhao, T. L., McKendry, I. G., Jaffe, D. A., and Lu, N. M.: Characterization of soil dust aerosol in China and its transport and distribution during 2001 ACE-Asia: 2. Model simulation and validation, *J. Geophys. Res.*, 108, 4262, doi:10.1029/2002JD002633, 2003.
- Han, Z. W., Ueda, H., Matsuda, K., Zhang, R. J., Arao, K., Kanai, Y., and Hasome, H.: Model study on particle size segregation and deposition during Asian dust events in March 2002, *J. Geophys. Res.*, 109, doi:10.1029/2004JD004920, 2004.
- Hanea, R. G., Velders, G. J. M., Segers, A. J., Verlaan, M., and Heemink, A. W.: A Hybrid Kalman Filter Algorithm for Large-

- Scale Atmospheric Chemistry Data Assimilation, *Mon. Wea. Rev.*, 135, 140–151, 2007.
- Houtekamer, P. L. and Mitchell, H. L.: Data assimilation using an ensemble Kalman filter technique, *Mon. Wea. Rev.*, 126, 796–811, 1998.
- Houtekamer, P. L. and Mitchell, H. L.: A sequential ensemble Kalman filter for atmospheric data assimilation, *Mon. Wea. Rev.*, 129, 123–137, 2001.
- Houtekamer, P. L., Mitchell, H. L., Pellerin, G., Buehner, M., Charon, M., Spacek, L., and Hansen, B.: Atmospheric Data Assimilation with an Ensemble Kalman Filter: Results with Real Observations, *Mon. Wea. Rev.*, 133, 604–620, 2005.
- Lorenc, A. C.: The potential of the ensemble Kalman filter for NWP – a comparison with 4D-Var, *Q. J. R. Meteorol. Soc.*, 129, 3183–3203, 2003.
- Liu, M. L., Westphal, D. L., Wang, S. G., Shimizu, A., Sugimoto, N., Zhou, J., and Chen, Y.: A high-resolution numerical study of the Asian dust storms of April 2001, *J. Geophys. Res.*, 108, 8653, doi:10.1029/2002JD003178, 2003.
- Lu, H. and Shao Y. P.: Toward quantitative prediction of dust storms: an integrated wind erosion modeling system and its application, *Environmental Modeling & Software*, 16, 233–249, 2001.
- Mitchell, H. L. and Houtekamer, P. L.: An Adaptive Ensemble Kalman Filter, *Mon. Wea. Rev.*, 28, 416–433, 2000.
- Mitchell, H. L., Houtekamer, P. L., and Pellerin, G.: Ensemble size, balance, and model error representation in an ensemble Kalman filter, *Mon. Wea. Rev.*, 130, 2791–2808, 2002.
- Mori, I., Nishikawa, M., Quan, H., and Morita, M.: Estimation of the concentration and chemical composition of kosa aerosols at their origin, *Atmos. Environ.*, 36, 4569–4575, 2002.
- Murayama, T., Sugimoto, N., Uno, I., Kinoshita, K., Aoki, K., Hagiwara, N., Liu, Z., Matsui, I., Sakai, T., Shibata, T., Arao, K., Shon, B. J., Won, J. G., Yoon, S. C., Li, T., Zhou, J., Hu, H., Abo, M., Iokibe, K., Koga, R., and Iwasaka, Y.: Ground-Based Network Observation of Asian Dust Events of April 1998 in East Asia, *J. Geophys. Res.*, 106, 18 345–18 359, 2001.
- Niu, T., Gong, S. L., Zhu, G. F., Liu, H. L., Hu, X. Q., Zhou, C. H., and Wang, Y. Q.: Data assimilation of dust aerosol observations for CUACE/Dust forecasting system, *Atmos. Chem. Phys. Discuss.*, 7, 8309–8332, 2007, <http://www.atmos-chem-phys-discuss.net/7/8309/2007/>.
- Park, S. U. and In, H. J.: Parameterization of dust emission for the simulation of the yellow sand (Asian dust) event observed in March 2002 in Korea, *J. Geophys. Res.*, 108, 4618, doi:10.1029/2003JD003484, 2003.
- Shao, Y.: A model of mineral dust emission, *J. Geophys. Res.*, 106, 20 239–20 254, 2001.
- Shao, Y. P., Yang, Y., Wang, J. J., Song, Z. X., Leslie, L. M., Dong, C. H., Zhang, Z. H., Lin, Z. H., Kanai, Y., Yabuki, S., and Chun, Y.: Northeast Asian dust storms: Real-time numerical prediction and validation, *J. Geophys. Res.*, 108, 4691, doi:10.1029/2003JD003667, 2003.
- Song, C. H. and Carmichael, G. R.: A three-dimensional modeling investigation of the evolution processes of dust and sea-salt particles in East Asia, *J. Geophys. Res.*, 106, 18 131–18 154, 2001.
- Sugimoto, N.: Network observations of Asian dust and anthropogenic aerosols with dual-polarization Mie-scattering lidars, *Proc. Int. Laser Radar Conf.*, 269–271, 2002.
- Sugimoto, N., Matsui, I., Shimizu, A., Uno, I., Asai, K., Endoh, T., and Nakajima, T.: Observation of dust and anthropogenic aerosol plumes in the Northwest Pacific with a two-wavelength polarization lidar on board the research vessel Mirai, *Geophys. Res. Lett.*, 29, 1901, doi:10.1029/2002GL015112, 2002.
- Sun, Y., Zhuang, G., Yuan, H., Zhang, X., and Guo, J.: Characteristics and sources of 2002 super dust storm in Beijing, *Chinese Science Bulletin*, 49, 698–705, 2002.
- Uematsu M., Wang, Z., and Uno, I.: Atmospheric input of mineral dust to the western North Pacific region based on direct measurements and a regional chemical transport model, *Geophys. Res. Lett.*, 30, 1342, doi:10.1029/2002GL016645, 2003.
- Uno, I., Amano, H., Emori, S., Kinoshita, K., Matsui, I., and Sugimoto, N.: Transpacific yellow sand transport observed in April 1998, *J. Geophys. Res.*, 106, 18 331–18 344, 2001.
- Uno, I., Wang, Z.F., Chiba, M., Chun, Y. S., Gong, S. L., Hara, Y., Jung, E., Lee, S.-S., Liu, M., Mikami, M., Music, S., Nickovic, S., Satake, S., Shao, Y., Song, Z., Sugimoto, N., Tanaka, T., and Westphal, D. L.: Dust model intercomparison (DMIP) study over Asia: Overview, *J. Geophys. Res.*, 111, D12213, doi:10.1029/2005JD006575, 2006.
- Vautard, R. and Blond, N.: Three-dimensional ozone analyses and their use for short-term ozone forecasts, *J. Geophys. Res.*, 109, D17303, doi:10.1029/2004JD004515, 2004.
- Wang, Z. F., Ueda, H., and Huang, M. Y.: A deflation module for use in modeling long-range transport of yellow sand over East Asia, *J. Geophys. Res.*, 105, 26 947–26 958, 2000.
- Wang, Z., Akimoto, H., and Uno, I.: Neutralization of soil aerosol and its impact on the distribution of acid rain over east Asia: Observations and model results, *J. Geophys. Res.*, 107, 4389, doi:10.1029/2001JD001040, 2002.
- Whitaker, J. S. and Hamill, T. M.: Ensemble Data Assimilation without perturbed observations, *Mon. Wea. Rev.*, 130, 1913–1924, 2002.
- Yumimoto, K., Uno, I., Sugimoto, N., Shimizu, A., and Satake, S.: Adjoint inverse modeling of dust emission and transport over East Asia, *Geophys. Res. Lett.*, 34, L08806, doi:10.1029/2006GL028551, 2007.
- Zhang, X. Y., Gong, S. L., Shen, Z. X., Mei, F. M., Xi, X. X., Liu, L. C., Zhou, Z. J., Wang, D., Wang, Y. Q., and Cheng, Y.: Characterization of soil dust aerosol in China and its transport and distribution during 2001 ACE-ASIA: Network observations, *J. Geophys. Res.*, 108, 4261, doi:10.1029/2002JD002632, 2003.